UCRL 2545
UNCLASSIFIED

UNIVERSITY OF CALIFORNIA

Radiation Laboratory

TWO-WEEK LOAN COPY

This is a Library Circulating Copy which may be borrowed for two weeks. For a personal retention copy, call Tech. Info. Division, Ext. 5545

BERKELEY, CALIFORNIA

DISCLAIMER

This document was prepared as an account of work sponsored by the United States Government. While this document is believed to contain correct information, neither the United States Government nor any agency thereof, nor the Regents of the University of California, nor any of their employees, makes any warranty, express or implied, or assumes any legal responsibility for the accuracy, completeness, or usefulness of any information, apparatus, product, or process disclosed, or represents that its use would not infringe privately owned rights. Reference herein to any specific commercial product, process, or service by its trade name, trademark, manufacturer, or otherwise, does not necessarily constitute or imply its endorsement, recommendation, or favoring by the United States Government or any agency thereof, or the Regents of the University of California. The views and opinions of authors expressed herein do not necessarily state or reflect those of the United States Government or any agency thereof or the Regents of the University of California.

Cy. 2

UCRL-2545
Unclassified-Chemistry Distribution

UNIVERSITY OF CALIFORNIA
Radiation Laboratory

Contract No. W-7405-eng-48

THE EFFECTS OF AGITATOR GEOMETRY IN THE MIXING OF LIQUID-LIQUID SYSTEMS

J. L. Fick, H. E. Rea and T. Vermeulen

April, 1954

Berkeley, California

TABLE OF CONTENTS

	Page
Abstract	3
Introduction	4
Experimental Program	7
Physical Variables Involved	7
Systems Investigated	8
Apparatus	8
Mixing Index Sampling System	10
Photoelectric Probes	10
Light Transmission Measurements	10
Power Measurements	11
Operating Procedure	11
Results and Discussion	13
Mean Drop Diameter or Specific Area	13
Coalescence	13
Effect of Volume Fraction of Dispersed Phase	14
Effect of Impeller Dimensions	14
Effect of Baffling	15
Power Requirements	16
Single-Phase Data	16
Two-Phase Data	17
Mixing Index Measurements	18
Definition of Mixing Index	19
Tentative Correlation of Experimental Results	19
Application	21
Conclusions	24
Appendix	25
Bibliography	26
Nomenclature	27
Tables	29
Figures	44

THE EFFECTS OF AGITATOR GEOMETRY IN THE MIXING OF LIQUID-LIQUID SYSTEMS

J. L. Fick*, H. E. Rea, and T. Vermeulen
Radiation Laboratory
and Department of Chemistry and Chemical Engineering
University of California, Berkeley, California

April, 1954

ABSTRACT

The effectiveness of mixing of two immiscible liquids may be expressed in terms of the interfacial area per unit volume of mixture. With four-bladed flat-paddle impellers of various proportions, in cylindrical tanks with "standard" baffling, the specific interfacial area is given by

$$A = \frac{72N^{1.2}L^{.8}\bar{\rho}^{.6}\phi}{\sigma^{.6}f_{\phi}},$$

confirming earlier work. The area is independent of impeller width over the range of the dimensionless ratio W/L from .133 to .65. This value of A is a maximum, and may be reduced by coalescence. In unbaffled tanks with other conditions the same, the specific area has been found to be approximately two-thirds the area in baffled tanks.

Power requirements for agitation of the systems studied are essentially the same as for a single liquid of equal mean density. The ratio of power in baffled and unbaffled vessels is about 3.2. Power requirements are found to be proportional to impeller width. The width used must be sufficient to produce bulk homogeneity of mixing. Mixing index as a measure of homogeneity is redefined, and its dependence on physical properties and geometrical variables is explored.

---

*Submitted in partial satisfaction of the requirements for the degree of Master of Science in Chemical Engineering. This work was done under the auspices of the Atomic Energy Commission.

INTRODUCTION

For some time the unit operation of the agitation of liquid-liquid systems as applied to solvent extraction and heterogeneous reactions has been a widely used but quantitatively little understood one. The present study, together with preceding ones,[9, 16, 19] was made to furnish a more quantitative insight into the problem of contact of two mutually insoluble liquids.

The bulk of investigations in the field of fluid agitation have been concerned with the power requirements for the operation.[3, 4, 12, 15, 17, 18, 20] Data on mass transfer in systems of solids suspended in liquids have been reported by Hixon and Baum,[6] Hixon and Wilkens,[8] and Mack and Marriner.[13] The necessity for a criterion of mixing intensity in such systems was recognized by Hixon and Tenney,[7] who conducted experiments on the suspension of solids in liquids. They proposed that the effectiveness of mixing could be represented by the approach to bulk homogeneity in the agitated system and termed this approach as the "mixing index" of the system.

Consideration of mass transfer operations in agitated two-phase liquid systems has been complicated by lack of knowledge of the extent of interfacial area in these systems. The criterion of mixing index is of little use as no conclusions can be drawn from it as regards the interfacial area. Because of the number of variables involved in mass transfer in this type of system, no correlation including all variables has been formulated. To further complicate the problem, the effect of the physical variables upon the over-all rate will change, depending on which transfer step controls. Since, for most mass transfer steps, the rate is given by the product of net molecular transfer across each unit area and the total interfacial area, it is clear that knowledge concerning the interfacial area in agitated liquid-liquid systems would contribute to a better understanding of mass transfer in these systems.

Most of the relating mean droplet diameters (a measure of

interfacial area) to the physical variables has been for the breakup of liquid jets in air.[1, 5, 10, 11, 14] Since this type of droplet formation involves physical variables not encountered in the dispersion of liquids in liquids in agitated vessels, the correlations set forth are of little use.

Clay[2] measured drop sizes in two-phase liquid systems in turbulent flow by the use of high speed photography. Although no firm correlation resulted from this work, Clay proposed that the drop diameter was related to the dimensionless Weber number:

$$We = \frac{N^2 L^3 \rho_c}{\sigma} \tag{1}$$

In work reported recently by Langlois, Gullberg and Vermeulen,[9] measurements of the light transmission of various transparent, non-colored, liquid-liquid emulsions were combined with high speed photographs of the unstable emulsions. The studies were made in a 10-inch cylindrical tank with a flat-bladed impeller at speeds of from 100 to 400 rpm and volume fractions of from 10 to 40 percent. It was shown by these investigators that there exists a straightforward relationship between the specific interfacial area of a two-phase liquid emulsion and the light transmission through this emulsion. This relation was expressed by the equation,

$$\frac{I_o}{I} = \beta A + 1 \tag{2}$$

for each system of one liquid dispersed in another. It was further shown that the value of the constant β in the equation was an empirical function of the ratio (m) of the refractive index of the dispersed phase to that of the continuous phase. A plot of β as a function of m yielded a smooth doubly branched curve with a discontinuity at m = 1.0. This relation was found to be independent of the volume fraction of dispersed phase and of mixing speed in the region covered in the studies.

It is evident that, with a properly calibrated photoelectric probe

for light transmission measurements, it is now possible to measure the specific interfacial area of any liquid-liquid emulsion provided both phases are colorless (non-absorbing). Vermeulen, Williams ans Langlois[19] have just reported data on drop diameters obtained by this method of measurement for a number of liquid-liquid and gas-liquid systems. For the liquid-liquid systems the specific interfacial area was related to the physical variables in the dimensionless form:

$$\frac{N^{1.2} d L^{.8} \bar{\rho}^{.6}}{\sigma^{.6} f_{\phi}} = 0.084 \qquad (3)$$

in combination with the relation between the specific area and the mean droplet diameter in the emulsion:

$$A = \frac{6\,\phi}{d} \qquad (4)$$

A common relation interrelating the two types of systems was derived and is given by:

$$\frac{N^2 d^{5/3} L^{4/3} \bar{\rho}/\sigma f_{\phi}^{5/3}}{(1 + 5.4 \cdot 10^{-6} d\sigma_c^{\rho} \mu_c/f_{\phi} \mu_D^3)^{1/3}} = 0.016 \qquad (5)$$

These investigations were conducted using paddle type impeller with four flat blades.

The study which resulted in these relationships was primarily concerned with the effects of fluid physical properties, impeller speed and dispersed phase volume fraction. The effects of agitator geometry were not explored.

Investigations into the effects of impeller geometry and baffling on mean drop diameter have been reported by Rea and Vermeulen.[16] In some systems disparities were encountered between these results and those reported by Vermeulen, Williams and Langlois.[19] It has since been proved that this was a result of the combination of coalescence in the systems a difference in probe location in the two studies.

EXPERIMENTAL PROGRAM

The present study was undertaken to extend the work initiated by the investigators just mentioned. The primary purpose was to study the effects of physical variables upon the specific interfacial area with the emphasis upon the variation of impeller geometry, tank size and baffling conditions.

The secondary objective was the investigation of power requirements in two phase liquid systems and the relation of these to the physical variables involved, with a view towards possible relation of power input to surface area produced.

The third objective was the relation of physical variables to the attainment of bulk homogeneity of mixing (100% mixing index) in the type of agitator which was employed in the present studies. Thus a knowledge of the effect of variables on interfacial area, power consumption and mixing index should supply a sound engineering basis for the solution of specific problems in agitation of two-phase liquid systems.

Physical Variables Involved.

The variables which were considered in the present studies were the following:

(1) The physical properties of the two liquids.

(2) Volume fraction of dispersed phase.

(3) Impeller speed.

(4) Agitator geometry: impeller length, impeller width, vessel diameter, vessel height, and baffling.

(The latter two factors were not varied independently of vessel diameter).

The range of physical properties was narrower than that covered in the precious work,[19] while the same ranges of volume fractions (10% to 40% dispersed phase) and of impeller speeds (100 to 400 rpm) were used. The ranges studied in the fourth set of variables listed above, will be discussed in detail in the section on apparatus. The emphasis in the present study was on these geometric variables.

Systems Investigated.

The liquids used in this study are set forth in Table 1 together with pertinent physical properties.

Apparatus.

The mixing vessels consisted of two cylindrical stainless steel tanks, the smaller of the two being approximately 10 inches in height and diameter, and the larger 20 inches in height and diameter.

The impellers were four-bladed flat paddles, and were centered vertically in all runs although their position could be varied. The dimensions of the tanks and impellers are given in Table 2. Impeller length or diameter was varied through a factor of 3 in the small tank and a factor of 1.5 in the large tank. This represents an overall variation of 6 in the quantity L in the correlation equation (3), since the longest impeller in the large tank was twice the length of that in the small tank. The ratio of impeller diameter to impeller width, L/W, was varied through a factor of 5.2 in the small tank and a factor of 2.1 in the large tank.

The tanks were fitted with four removable vertical baffles, one-tenth the tank diameter in width, spaced at equal intervals around the tank wall and perpendicular to it.

Figure 1 shows a drawing of the two tanks mounted in the steel frame. The ten-inch tank was suspended and removable from its cover. The cover was attached to the frame by means of an integral suspension ball bearing unit to which it was welded. A spindle assembly with two sets of ball bearings connected to the impeller shaft was contained in a collar welded to the upper side of the frame. This method of assembly allowed the tank cover and impeller shaft to rotate independently of each other, and enabled the power input to be determined by torque measurement on the tank.

The tank was fastened to the suspended cover by means of wing nuts and L-shaped bolts. The vessel was made liquid- and air-tight by use of a cork gasket around the edge of the cover and a mercury seal on the impeller shaft. Fittings on the ten-inch tank consisted

of an opening in the cover for mounting the light-transmission probe, two 1/4-inch N. P. S. tapped holes for feed lines and a 1/8-inch N. P. S. tapped hole for either a vent or thermometer. These fittings were placed centrally between baffles. The bottom of the tank was also fitted with a 1/2-inch N. P. S. outlet located in the center.

The cover of the twenty-inch tank was suspended similarly to that of the small tank, which allowed independent rotation of the cover and impeller shaft. Due to the size of this unit, the tank was also fitted with a ball thrust bearing assembly at the bottom. The cover and impeller-shaft assembly unit was so designed that it could be lifted from the tank. The steel channel supporting the cover was also attached to a post in a mounting that was secured to the bottom of the frame. The cover was lifted, after the sealing bolts were unfastened, by sliding the post upward in the mounting. It was held in the upper position by a spring-loaded stop, which snapped under the bottom of the supporting post. In this way the cover-and-shaft unit could be swung free for changing impellers.

The fittings in the cover on the twenty-inch tank consisted of a fitting with a seal to receive the adjustable height light transmission probe, two 1/2-inch N. P. S. feed holes and a 1/4-inch N. P. S. vent hole. A 1/2-inch drain line was located at the tank bottom in the center. Gasketing and mercury seal were similar to those in the ten-inch tank.

Impellers in both tanks were driven by means of a V-belt drive connected to a 3/4 horsepower, 3-phase, 60-cycle, 220-volt, 216-rpm right angle ring mounted gear motor supplied by Electra Motors, Inc. V step-cone pulleys mounted on each of the impeller shafts and on the motor shaft allowed the impellers to rotate at 94, 154, 247, and 394 rpm.

A portion of the investigations were made using the ten-inch tank described by Vermeulen, Williams and Langlois.[19] The important differences in this apparatus were the drive which allowed smaller increments in varying the stirring speed, and the placement of the photoelectric probe whose gap was opposite the impeller dip.

A coil of 1/4-inch O. D. copper tubing was soldered to the outside

of each tank to provide temperature control by circulation of cooling water.

Mixing Index Sampling System.

The ten-inch tank was proveded with two stainless steel tubes (0.075-inch I.D.) which were inserted through Teflon seals in the two 1/2-inch holes in the cover. For withdrawal of samples, a 16-gauge hypodermic needle was pressed into the tube end protruding above the Teflon seal and samples were taken by means of a 20 cc hypodermic syringe. The lower part of each tube was bent to allow sampling at the center or at the wall of the tank. Figure 8 shows the position of the six sampling points.

Photoelectric Probes.

The photoelectric probes used in this study were of the design described in detail by Langlois, Gullberg and Vermeulen.[9] All the probes were similar in internal geometry. Probe No. 1 however, differed from probes 2, 3 and 4 in external construction. A diagram of probes 2, 3, and 4 is shown in Figure 2. Probes 2 and 3 were machined from stainless steel and had surfaces of moderately high reflectivity, while probe 4 was made from mild steel which was treated by application of a dull black finish to eliminate this reflectivity. The calibration curve for the probes, Figure 3, shows the effect of the reflecting surfaces in reducing the light extinction in probes 2 and 3 as compared to that of probes 1 and 4.

Light Transmission Measurements.

The circuits used in measuring the light transmission of emulsions were identical with those described by Vermeulen, Williams, and Langlois.[19] The light source was kept at a constant value by means of a bridge arrangement utilizing a Leeds and Northrup student potentiometer. The volage input to the light source was controlled by intermittent manual adjustment of the bridge circuit. The photocell circuit involved a 90 volt d.c. input, a Leeds and Northrup galvanometer, Cat. No. 2430D and an RCA photocell No. 1P41. The current measured by the galvanometer was proportional to the intensity of the light impinging upon the photocell.

Power Measurements.

Power requirements in the systems studied were measured by using the tank as part of a dynamometer. The force required to keep the tank from turning in the direction of impeller rotation was measured by a Toledo Scale, Model 4021-BA, connected by a cord over a nearly frictionless pulley to a stud in the tank cover. Scale readings were found to be reproducible within 0.03-0.04 lb. Experiments with the tank empty of liquid indicated negligible torque due to the mercury seal.

Operating Procedure.

The procedure for obtaining light transmission measurements in the emulsions studied has been described in detail in three previous investigations[9, 16, 19] and will not be discussed here. As noted by these investigators the light transmission indicated by current readings was not a steady value. The fluctuations however were of such short time length that an average could be taken as a fairly reliable value. The condition previously encountered, and explained as irreproducibility of emulsification again occurred. A deviation of ± 5% from a smooth curve drawn through the light transmission values is combined with an uncertainty of ± 10% in the probe calibration.

In the runs where power was measured the next step was the reading and recording of the force measured by the Toledo Scale. This reading fluctuated rapidly, with a greater variation observed the higher the mixing speed. This variation amounted to approximately 5% at the highest speed, and a series of force readings (between ten and twenty) was taken for averaging, to calculate the torque exerted and the power consumed.

In cases where mixing index was obtained, ten cc samples were taken from the points indicated in Figure 8. The volume of dispersed phase was recorded for each sample after the two phases had settled till each was clear. For check purposes, two or three samples were taken at each point. The material withdrawn in the samples was returned to the tank after being measured, in order to avoid relative

depletion of either phase, and possible admixture of air. A series of samples taken over a period of time indicated that the rate of reaching the ultimate value of mixing index was too fast to be observed. In nearly all cases, check samples agreed within 3 or 4 percent. Although samples were withdrawn only from the top half of the tank, it is believed that the results give an accurate indication of the relative approach to bulk homogeneity.

RESULTS AND DISCUSSION

Mean Drop Diameter or Specific Area

Of the impellers used in the present investigation, listed in Table 1, numbers A4 and B4 correspond to those used in the initial investigation.[19] The mean drop diameters obtained and the corresponding impellers and speeds are set forth in Table 3.

Coalescence

As mentioned earlier, disparities encountered in some instances between the initial results[19] and those obtained with the modified apparatus[16] have proved to be due to the differences in probe location, combined with a tendency for some mixtures to coalesce rapidly. The magnitude of this effect is probably greatest in mixtures of methyl isobutyl ketone and water, and is shown by the following values obtained at 20 volume percent methyl isobutyl ketone with impeller A4.

N	d. cm.	
rev/sec	Probe 1*	Probe 2**
1.57	.0429	.0667
2.57	.0285	.0485
4.12	.0173	.0302
6.57	.0096	.0182

* From Table 3
** From Reference (16)

The quantitative effect of physical variables upon the rate of coalescence is beyond the scope of the present study, but is evidently a major unsolved factor in characterizing the degree of dispersion throughout a mixing vessel. Those systems studied with probes 2 and 4, for which results are given in Table 3, are selected because of their apparent lack of coalescence; that is, their drop diameters measured with probe 1 and with probe 2 agree closely. For these systems, the drop diameter represents both the maximum and the average degree of dispersion. For methyl isobutyl ketone-water mixtures, on the other hand, they represent only the maximum degree of dispersion.

Effect of Volume Fraction of Dispersed Phase.

The observed values of mean drop diameter for each system and speed were found to increase with volume fraction, in agreement with the empirical behavior found previously.[19] The diameters at different values of ϕ can be compared with those at $\phi = 0.1$ by use of the relation:

$$d_{.1} = d/f\phi \qquad (6)$$

The following values of the volume fraction function have been used for computing the values of $d_{.1}$ given in Table 3.

ϕ	f_ϕ
0.10	1.00
0.20	1.25
0.30	1.51
0.40	1.76

The individual values used to obtain the average values of f_ϕ are set forth in Table 4.

It may be noted that the function is nearly linear in ϕ. The present results indicate that it does not depend upon any one set of impeller proportions, but applies generally, for the range of impeller dimensions used.

Effect of Impeller Dimensions.

The mean drop diameter is found to depend on the impeller diameter L, and to be independent of impeller width W. The results obtained previously, summarized in Equation (3)

$$\frac{N^{1.2} d\, L^{.8}\, \bar{\rho}^{\,.6}}{\sigma^{.6} f_\phi} = .084$$

contained implicitly (L/W) raised to an unknown power. In the present study, L was varied from 5 to 15 inches and L/W from 1.5 to 8.0. The

results indicate that Equation (3) should not contain W, and, as written, is widely applicable to baffled systems with flat-paddle impellers. Although further experimental study will be needed to confirm this point, it appears likely that the number of impeller blades also is without effect, provided always that agitation is sufficiently intense to insure bulk homogeneity.

A graphical demonstration of these results is given in Figure 4, in which the solid line corresponds to Equation (3). The deviation from this line is only slightly greater than that experiences with a single impeller geometry.[19]

Effect of Baffling.

Runs without baffling were made in the 10-inch tank with impeller A4 on four of the five systems investigated under baffled conditions. Without exception, the mean drop diameters in the unbaffled tank were larger than the corresponding values in the baffled tank. An average ratio of diameters was calculated for each system as follows:

System	(d, unbaffled)/(d, baffled)
$MiBK/H_2O$	1.65
CCl_4/H_2O	1.63
$i\ C_8/H_2O$	1.79
$H_2O/MiBK$	1.56 (weighted 2)

The average of these ratios, 1.64, may be used for tentative correlation, and leads to the relation,

$$\frac{N^{1.2}\, d\, L^{.8}\, \bar{\rho}^{\,.6}}{\sigma^{.6}\, f_{\phi}} = .138 \qquad (7)$$

for the minimum mean drop diameter in unbaffled tanks. Figure 5 shows the data for unbaffled tanks on a plot of d/Lf_{ϕ} vs. Weber number. The solid curve is based upon the numerical value estimated for Equation (7),

and the dashed curve given for comparison is taken from the baffled-tank data of Figure 4.

Power Requirements.

Single-Phase Data. Power measurements reported by Rea and Vermeulen[16] have been subjected to further interpretation, and will be discussed here. The power requirements for mixing were calculated from torque measurements by the familiar equation for brake horsepower:

$$P = 2\pi \tau N F \tag{8}$$

The original data, which can be found in the cited reference, involved the following liquids and impellers:

Liquid	Tank	Impellers
Water	20-inch, baffled	B2, B3, B4
Water	10-inch, baffled	A2, A3, A4
CCl_4	" "	"
Water	" "	"
CCl_4	10-inch, unbaffled	A2, A3, A4
MiBK	" "	"

Power requirements are usually correlated in terms of a dimensionless power number $Pg/N^3L^5\rho$, which is known to depend upon the agitator geometry. In order to determine the effect of paddle width, W, upon power, the length-width ratio L/W is plotted against this power number for all the systems measured. This plot is shown in Figure 6. A slope of -1 results, indicating that a power group, P_o, can be defined as

$$P_o = Pg_c/N^3L^4 W \rho \tag{9}$$

For baffled systems with four-bladed flat paddles in tanks with $H \cong T$, $P_o = 20.4$. For similar systems without baffling, $P_o = 6.3$.

Two Phase Data.

Rea and Vermeulen[16] measured the power consumption during agitation of following mixtures:

Mixture	Tank	Impellers
iC_8 - H_2O	A (baffled)	4
CCl_4 - H_2O	A "	4
CS_2 - H_2O	A "	2, 3, 4
n-BuOH-H_2O	A "	2, 3, 4
MiBK - H_2O	A "	2, 3, 4
MiBK - H_2O	B "	1, 2, 3, 4
MiBK - H_2O	A (unbaffled)	2, 3, 4
CS_2 - H_2O	A "	2, 3, 4
CCl_4 - H_2O	A "	4

In addition, power measurements have been made on the following systems during the present study:

Mixture	Tank	Impellers
CCl_4 - H_2O	A (baffled)	2, 3, 4
MiBK - H_2O	B (unbaffled)	1, 2, 3, 4
MiBK - H_2O	A (baffled)	3

These later data are presented in Table 5, and although the results appear less accurate they are in qualitative agreement.

It is well known that the power requirements for gas-liquid mixtures are substantially less than those for pure liquids of the same mean density.[3,4] Moreover, Long[12] observed a small deviation from linear behavior for liquid-liquid mixtures in unbaffled tanks. However the present reqults indicate that any such deviations are negligible for design purposes, and that the power group of Equation (9) can be used by taking ρ to be the bulk mean density:

$$\rho_m = \rho_C + (\rho_D - \rho_C)\,\phi \tag{10}$$

Figure 7 illustrates the behavior of mixtures for two systems, carbon tetrachloride - water and n-butanol water. In order to show the effect of density the ordinate is taken as $P_o \times \rho_m$ with ρ_m in metric units; that is, as Pg_c/N^3L^4W. The intercepts are seen to be proportional to the densities of the pure phases for both the unbaffled and baffled tanks. Moreover, the plots are essentially linear in ϕ, as is ρ_m. This appears to justify the use of the same power-group correlation as for homogeneous liquids.

The power results for the unbaffled tank enable the conclusion to be drawn that, for given impeller and tank geometry and a stipulated system and mean drop diameter, the power required is very nearly the same in a baffled and in an unbaffled tank. By combination of Equations (3) and (7) with equal values of d, L and other physical variables,

$$\frac{(N)_{unbaffled}}{(N)_{baffled}} = 1.64^{1/1.2} \tag{11}$$

By use of the power relation

$$\frac{(P)_{unbaffled}}{(P)_{baffled}} = \frac{6.3}{20.4} \times \left[\frac{N_{unbaffled}}{N_{baffled}}\right]^3$$

$$= \frac{6.3}{20.4} \times (1.64)^{2.5}$$

$$= 1.06$$

which is not significantly different from unity.

Mixing Index Measurements.

The approach to bulk homogeneity was studied in the following mixtures with specified agitation conditions in the 10-inch baffled tank:

Mixture	Impeller
MiBK in H_2O	A1, A2
H_2O in MiBK	" "
H_2O in CCl_4	A2, A3, A4

Definition of Mixing Index.

The method of characterizing mixing index is a variation of that suggested by Hixon and co-workers. In both methods the over-all mixing index, I_m, is computed as the average of several point values, i_m. In Hixon's method, each point value of the mixing is given by the ratio of a local volume-fraction of a phase, ϕ_s, to the mean volume-fraction of that phase, ϕ, calculated for whichever of the two phases gives a point value below 100 percent. This method has appeared unsatisfactory for values of mean volume-fraction that are substantially below 0.50, in that a given deviation (say one percent by volume) below the mean will yield a much larger deviation from 100 percent than the same deviation above the mean. It appears preferable to define an arbitrary function that has a continuous slope in the vicinity of 100 percent mixing index, but otherwise possesses similar properties to Hixon's mixing index.

A mixing number (M. N.) may be defined such that

$$\frac{200 - \text{M. N.}}{\text{M. N.}} = \frac{(1 - \phi_s)\phi}{\phi_s (1 - \phi)} \qquad (12)$$

Under this definition, the mixing number will range from zero to 200. The point mixing index in percent, i_m, is then defined as equal to either M. N. or 200-M. N. whichever is less than 100. The resulting values of mixing index are shown in Figure 9, which can be used directly without further recourse to Equation (12).

Tentative Correlation of Experimental Results.

The values of I_m, obtained by this method for the runs listed above, are given in Table 6. A tentative correlation of these results has been

obtained by consideration of the Newtonian settling velocity under turbulent conditions; together with the consideration that this settling velocity should bear a constant ratio to the peripheral velocity, NL, of the impeller (at a constant W). Thus, the dimensionless group

$$NL \left[\rho_m / |\rho_D - \rho_m| g\, d\right]^{.5} \tag{13}$$

should be a constant for a given tank geometry; that is, for given proportions of tank and impeller regardless of actual size. If d is eliminated between this group and Equation (3), the following dimensionless group results which will be called the settling group:

$$\frac{N^{1.6}\, L^{1.4}\, \rho_m^{.5}}{(|\rho_D - \rho_m|\, g\, f\, \phi)^{.5}\, (\sigma/\bar{\rho})^{.3}} \tag{14}$$

A plot of the I_m values from Table 6, on a probability scale, against this group on a logarithmic scale, was found to give a straight-line relation for all the values of ϕ (between 0.1 and 0.4) with any one impeller.

Next, various combinations of L/T, W/H and L/W were tested. It was found that the ratio, LW/TH, which will be called the geometrical group, collected the data into a single correlation. It must be noted however, that T and H have not been varied independently. Figure 10 is a plot, on a logarithmic coordinates, of the geometrical group against the settling group. The line drawn through the points has a minus one slope, suggesting that the group characterizing mixing index should be

$$M = \frac{N^{1.6}\, L^{2.4}\, W\, \rho_m^{.5}}{(|\rho_D - \rho_m|\, g\, f_\phi)^{.5}\, (\sigma/\bar{\rho})^{.3}\, TH} = \text{const.} \tag{15}$$

Figure 11 shows a probability-logarithmic plot of mixing index vs. M for the four impeller geometries and the three mixtures investigated. The threshold of complete homogeneity, for practical purposes,

may be said to occur at a mixing index of 95 percent. The corresponding value of M, as read from this plot and applicable for the particular conditions of measurement, is 1.4.

The present mixing-index group, M, is suggested only as a highly tentative basis for correlating this type of data. The data on which it is based are few, and of limited accuracy. Viscosity has not been investigated as a significant variable, and there is evidence from the literature that M may be inversely proportional to a small power (0.1 to 0.2) of the bulk Reynolds number. Nevertheless, the treatment presented is believed to point the way toward an ultimate accurate correlation of bulk mixing.

Application.

For systems which do not coalesce rapidly, a knowledge of the effect of geometrical factors upon drop diameter, power consumption and mixing index together is sufficient to draw important tentative conclusions for equipment design. It may be assumed that a given flow rate is specified for an actual mixing installation. A tank volume is assumed, and a given drop diameter is then required in order to achieve the desired reaction or mass-transfer in the established residence time. Equation (3) then fixes the following product:

$$N^{1.2} L^{.8} = \text{const.} \qquad (16)$$

Likewise, it is wasteful to mix more intensely than will just produce bulk homogeneity, as characterized by a 95 percent mixing index. From Equation (15), for assumed tank dimensions T and H,

$$N^{1.6} L^{2.4} W = \text{const.} \qquad (17)$$

It is also desired that the power input be a minimum to produce the specified homogeneity and dispersion. From Equation (9),

$$N^{3} L^{4} W = \text{a minimum} \qquad (18)$$

The restrictions placed upon the system by Equations (16), (17) and (18) result in the following important relations:

$$N = \text{a maximum} \tag{19}$$

$$L = \text{a minimum} \tag{20}$$

$$W = \text{maximum} \tag{21}$$

Application of these relations must be governed by the limits of the variables in this investigation. These relations can be graphically illustrated by a simple example. Let us consider a set of conditions which result in the following values for the two products which are to be held constant.

$$N^{1.2} L^{.8} = 10$$

$$N^{1.6} L^{2.4} W = 1000$$

These values were picked because they results in the simple expression

$$N = \sqrt{W},$$

and the reasoning involved is valid for any possible value of the two groups. Tabulation of the individual values below demonstrates the results in Equations (19), (20) and (21).

W	N	L	$N^3 L^4 W$
1	1	17.8	100,000
2	1.414	10.6	71,300
3	1.732	7.8	57,700
4	2	6.3	49,500
5	2.236	5.3	44,600

Of course the relations derived must be applied together with considerations of the limitations of equipment, but these results point the way to a firm theoretical basis for the design of agitation equipment for the contact of mutually insoluble liquids in mass transfer and heterogeneous reaction processes.

CONCLUSIONS

(1) The use of a properly calibrated photoelectric probe for the measurement of light transmission through emulsions of non-absorbing (colorless) liquids provides a rapid measurement of interfacial area in agitated liquid-liquid systems.

(2) The interfacial area in liquid-liquid systems mixed in vessels of different size but similar proportions is dependent upon the impeller diameter, stirring speed, volume fraction of dispersed phase, density of each phase and interfacial area produced.

(3) The conclusions of section 2 as applied to the entire vessel volume are valid only for systems which do not undergo coalescence which results in larger drops than those produced at the impeller tip. The correlation for drop size holds for these coalescing systems but only at the point of highest turbulence in the vessel.

(4) In stirred cylindrical vessels with flat bladed paddle-type impellers and tank height approximately equal to tank diameter, the power requirements depend on the stirring speed, impeller diameter and impeller width.

The power input for the mixing of two-phase liquid systems is the same as that in a single liquid of equal mean density, and further, the power required to produce a given amount of interfacial area is the same in baffled and unbaffled tanks.

(5) The achievement of bulk homogeneity of mixing (100% mixing index) is dependent upon mixing speed, impeller diameter, impeller width, tank height, tank diameter, emulsion droplet size and density difference between the two liquid phases. It must be reiterated that the dependence on these variables is tentative due to the fact that only limited data were used to formulate the correlation. The effect of viscosity upon the achievement of bulk homogeneity has not been investigated and is suggested as a subject for furture study.

(6) The results from which the above conclusions are drawn offer a sound engineering basis for the design of an agitation system for the contact of two immiscible liquids for purposes of solvent extraction or heterogeneous reaction.

APPENDIX

BIBLIOGRAPHY

1. R. A. Castleman, Jr., Bur. Standards J. Research 6, 369 (1931).
2. P. H. Clay, Proc. Acad. Sci. Amsterdam 43, 852, 979 (1940).
3. C. M. Cooper, G. A. Fernstrom, and S. A. Miller, Ind. Eng. Chem., 36, 504 (1944).
4. H. G. Foust, D. E. Mack, and J. H. Rushton, Ind. Eng. Chem. 36, 517 (1944).
5. A. Haenlein, T. M. No. 659, Nat. Advisory Comm. Aeronaut. (1931).
6. A. W. Hixon, and S. J. Baum, Ind. Eng. Chem. 33, 478 (1941).
7. A. W. Hixon, and A. H. Tenney, Trans. Am. Inst. Chem. Engrs. 31, 113 (1935).
8. A. W. Hixon, and G. A. Wilkens, Ind. Eng. Chem. 25, 1196 (1933).
9. G. E. Langlois, J. E. Gullbert, and T. Vermeulen, J. Sci. Instr. (In press)
10. D. W. Lee, and R. C. Spencer, T. R. No. 454, Nat. Advisory Comm. Aeronaut. (1933).
11. H. C. Lewis, D. G. Edwards, M. J. Goglia, R. I. Rice, and L. W. Smith, Ind. Eng. Chem. 40, 67 (1948).
12. R. S. Long, M. S. Chem. Eng. Thesis, University of California (1949).
13. D. E. Mack, and R. A. Marriner, Chem. Engr. Prog. 45, 545 (1949).
14. A. C. Merrington, and E. G. Richardson, Proc. Phys. Soc. 59, 1 (1947).
15. R. B. Olney, and G. J. Carlson, Chem. Engr. Prog. 43, 473 (1947).
16. H. E. Rea, and T. Vermeulen, Univ. Calif. Radiation Laboratory Report No. UCRL-2123 (Unclassified), April, 1953.
17. J. H. Rushton, Chem. Engr. Prog. 48, 33 (1952); 48, 95 (1952).
18. J. H. Rushton, E. W. Costich, and H. J. Everett, Ibid. 46, 395 (1950).
19. T. Vermeulen, G. M. Williams, and G. E. Langlois. (In press)
20. A. M. White, and A. D. Summerford, Ind. Eng. Chem. 25, 1025 (1933).

NOMENCLATURE

Latin Letter Symbols

A = specific area = total interfacial area per unit volume, cm^2/cm^3.

A1, A2, A3, A4, A5, A6 = 10" tank impellers; see Table 1.

B2, B3, B4 = 20" tank impellers; see Table 1.

d = mean drop diameter, cm.

$d_{.1}$ = mean drop diameter at ϕ = .1, cm.

d_ϕ = mean drop diameter at ϕ, cm.

F = force measured by Toledo scale in dynamometer measurement of power, lb.

f_ϕ = drop diameter-volume fraction function = $d_\phi/d_{.1}$ dimensionless.

g = gravitational constant.

H = tank height, cm. and in.

I = light transmission through emulsion.

I_o = light transmission through continuous phase alone.

I_o/I = light extinction ratio.

I_m = over-all mixing index in agitated tank, %.

i_m = point value of mixing index, %.

L = impeller diameter, cm. and in.

M = group characterizing mixing index; see Equation (14), dimensionless.

m = refractive index ratio, n_d/n_c.

M.N. = mixing number; see Equation (12), dimensionless.

N = stirring speed, rpm or rps.

n_c = refractive index (n_D^{20}) of continuous phase.

m_d = refractive index (n_D^{20}) of discontinuous phase.

P = power, ft-lbs/sec.

P_o = power number = $Pg/N^3L^5W\rho$, dimensionless.

r = lever arm for dynamometer measurement of power, ft. or in.

T = tank diameter, cm. and in.

W = impeller blade width, cm. and in.

We = Weber number = $N^2 L^3 \rho_c/\sigma$, dimensionless.

Greek Letter Symbols.

β = proportionality constant in Equation (2) relating I_o/I and A.

μ_c = viscosity of continuous phase, gm/cm-sec.

μ_d = viscosity of discontinuous phase, gm/cm-sec.

ρ_c = density of continuous phase, gm/cm^3, lb/ft^3.

ρ_d = density of discontinuous phase, gm/cm^3, lb/ft^3.

ρ_m = volume fraction mean density = $\rho_c + (\rho_d - \rho_c)\,\phi$ gm/cm^3, lb/ft^3.

$\bar{\rho}$ = effective density for drops = $.6\rho_d + .4\rho_c$ gm/cm^3, lb/ft^3.

σ = interfacial tension, dynes/cm.

ϕ = over-all volume fraction of dispersed phase.

ϕ_s = point value of volume fraction of dispersed phase.

Table I

PHYSICAL PROPERTIES OF LIQUIDS USED IN MIXING STUDIES[1]

Liquid	Refractive Index n_D^{20}	Density gm./cm^3	Viscosity cp.	Interfacial Tension[2] dynes/cm.
Distilled Water	1.3330	.998	1.00	---
Carbon Tetrachloride	1.4590	1.595	.99	38.0
Kerosene	1.4446	.871	1.81	22.8
Iso-Octane (2, 2, 4-trimethyl pentane)	1.3920	.693	.517	41.0
Methyl Iso-Butyl Ketone	1.3957	.800	.585	12.0

(1) All properties measured at 20°C.

(2) Interfacial tension with water as the other phase.

Table 2

DIMENSIONS OF MIXING APPARATUS
(Inches)

	10" Tank (A)	20" Tank (B)
Tank Height	8.87	20.0
Tank Diameter	10.35	20.0
Baffle Width	1.00	2.00
Diameter of Impeller No. 1	2.50	
Width of Impeller No. 1	.94	
Diameter of Impeller No. 2	5.00	10.00
Width of Impeller No. 2	.94	2.00
Diameter of Impeller No. 3	7.50	15.00
Width of Impeller No. 3	.94	2.00
Diameter of Impeller No. 4	6.77	13.00
Width of Impeller No. 4	1.65	3.72
Diameter of Impeller No. 5	5.00	
Width of Impeller No. 5	2.80	
Diameter of Impeller No. 6	6.77	
Width of Impeller No. 6	4.40	
Lever arm for dynamometer measurements (r)	5.75	11.25
Number of Baffles	4	4
Number of Blades on all impellers	4	4

Table 3

MEAN DROP DIAMETERS IN LIQUID-LIQUID SYSTEMS

ϕ	N RPS	$\frac{I_o}{I}$	d cm.	d/f_ϕ cm.	$\frac{N^2L^3\bar{\rho}}{\sigma}$	$\frac{N^{1.2}dL^{.8}\bar{\rho}^{.6}}{f_\phi\ \sigma^{.6}}$
		Probe 3		CCl_4 in H_2O	Impeller B4	
.20	1.57	6.34	.0116	.0092	3460	.0371
	2.37	9.31	.0075	.0060	7880	.0407
.40	1.57	6.82	.0214	.0122	3460	.0491
	2.37	11.10	.0124	.0071	7880	.0466
		Probe 3		CCl_4 in H_2O	Impeller B3	
.20	1.57	5.48	.0139	.0110	4920	.0474
	2.43	9.67	.0072	.0057	11750	.0413
.41	1.57	7.35	.0201	.0115	4920	.0495
	2.43	12.30	.0113	.0065	11750	.0470
		Probe 2		CCl_4 in H_2O	Impeller A4	
.20	2.57	3.62	.0238	.0189	1170	.0760
	4.12	6.50	.0113	.0090	3020	.0640
	6.57	8.94	.0079	.0062	7620	.0768
.40	2.57	4.65	.0342	.0195	1170	.0780
	4.12	8.06	.0176	.0101	3020	.0716
	6.57	11.00	.0125	.0071	7620	.0880
		Probe 2		CCl_4 in H_2O	Impeller A3	
.10	2.57	2.76	.0177	.0177	1550	.0760
	4.12	4.57	.0087	.0087	4000	.0662
	6.57	6.00	.0062	.0062	10100	.0820
.20	2.57	4.17	.0197	.0157	1550	.0675
	4.12	6.52	.0113	.0090	4000	.0685
	6.57	8.29	.0086	.0068	10100	.0900
.30	2.57	4.92	.0238	.0158	1550	.0680
	4.12	8.00	.0133	.0088	4000	.0670
	6.57	10.20	.0101	.0067	10100	.0887
		Probe 4		CCl_4 in H_2O	Impeller A2	
.10	4.12	6.51	.0098	.0098	1260	.0560
	6.57	9.92	.0061	.0061	3190	.0605
.20	4.12	9.61	.0125	.0099	1260	.0565
	6.57	13.40	.0087	.0069	3190	.0685
.30	4.12	10.40	.0173	.0114	1260	.0650
	6.57	14.10	.0123	.0082	3190	.0815

Table 3
(continued)

ϕ	N RPS	$\frac{I_o}{I}$	d cm.	d/f_ϕ cm.	$\frac{N^2L^3\bar{\rho}}{\sigma}$	$\frac{N^{1.2}dL^{.8}\bar{\rho}^{.6}}{f_\phi\ \sigma^{.6}}$
		Probe 4		CCl_4 in H_2O		Impeller A5
.10	4.12	5.76	.0113	.0113	1260	.0646
	6.57	9.85	.0061	.0061	3190	.0605
.20	4.12	8.67	.0141	.0112	1260	.0641
	6.57	12.70	.0092	.0073	3190	.0725
.30	4.12	9.68	.0186	.0123	1260	.0705
	6.57	14.60	.0119	.0079	3190	.0785
		Probe 4		Iso-Octane in H_2O		Impeller A5
.10	2.57	1.52	.0438	.0438	269	.100
	4.12	2.12	.0203	.0203	693	.0814
	6.57	2.79	.0128	.0128	1750	.0800
.20	2.57	2.08	.0423	.0336	269	.0761
	4.12	3.52	.0180	.0146	693	.0573
	6.57	4.81	.0120	.0095	1750	.0661
.30	2.57	2.56	.0439	.0290	269	.0657
	4.12	4.43	.0200	.0132	693	.0530
	6.57	6.57	.0122	.0081	1750	.0564
		Probe 4		Iso-Octane in H_2O		Impeller A4
.098	2.57	1.86	.0260	.0260	670	.0748
	4.12	3.47	.0091	.0091	1720	.0460
	6.57	6.06	.0044	.0044	4350	.0390
.20	1.57	1.86	.0534	.0424	250	.0675
	2.57	2.84	.0249	.0198	670	.0570
	4.12	5.96	.0092	.0073	1720	.0370
	6.57	8.07	.0065	.0052	4350	.0460
		Probe 4		Iso-Octane in H_2O		Impeller A3
.10	2.57	2.06	.0215	.0215	936	.0683
	4.12	3.24	.0102	.0102	2410	.0575
	6.57	4.37	.0068	.0068	6100	.0666
.20	2.57	2.83	.0290	.0230	936	.0730
	4.12	4.85	.0119	.0095	2410	.0535
	6.57	6.36	.0085	.0068	6100	.0666
.30	2.57	3.97	.0230	.0152	936	.0483
	4.12	6.23	.0130	.0086	2410	.0485
	6.57	8.28	.0094	.0062	6100	.0607

Table 3

(3)

ϕ	N RPS	$\frac{I_o}{I}$	d cm.	d/f_ϕ cm.	$\frac{N^2L^3\bar{\rho}}{\sigma}$	$\frac{N^{1.2}dL^{.8}\bar{\rho}^{.6}}{f_\phi\ \sigma^{.6}}$
		Probe 3 Methyl Iso-Butyl			Ketone in H_2O	Impeller B2
.10	1.57	1.84	.0157	.0157	2740	.0712
	2.57	2.00	.0132	.0132	7320	.1080
	4.12	2.35	.0098	.0098	18900	.1410
	5.33	2.80	.0074	.0074	31600	.1450
.40	1.57	2.70	.0311	.0177	2740	.0804
	2.57	3.12	.0248	.0142	7320	.1160
	4.12	4.06	.0173	.0099	18900	.1430
	5.33	5.30	.0122	.0070	31600	.1370
		Probe 4 H_2O in Kerosene				Impeller A3
.10	2.57	4.59	.0200	.0200	1860	.0960
	4.12	7.05	.0119	.0119	4790	.101
	6.57	9.65	.0083	.0083	12100	.122
.20	2.57	6.67	.0254	.0202	1860	.0969
	4.12	10.30	.0155	.0123	4790	.104
	6.57	13.10	.0119	.0094	12100	.138
.30	2.57	7.87	.0314	.0208	1860	.0996
	4.12	11.50	.0206	.0136	4790	.115
	6.57	14.70	.0158	.0104	12100	.153
		Probe 4 H_2O in Kerosene				Impeller A5
.10	2.57	3.67	.0269	.0269	550	.0935
	4.12	5.78	.0151	.0151	1420	.0925
	6.57	9.15	.0088	.0088	3600	.0944
.20	2.57	4.86	.0373	.0296	550	.1030
	4.12	8.12	.0202	.0160	1420	.0980
	6.57	11.65	.0135	.0107	3600	.1150
.30	2.57	5.55	.0475	.0315	550	.1090
	4.12	9.40	.0257	.0170	1420	.1040
	6.57	13.00	.0180	.0119	3600	.1280
		Probe 1 Methyl Iso-Butyl			Ketone in H_2O	Impeller A4
.10	1.57	1.85	.0300	.0300	945	.106
	2.07	2.02	.0250	.0250	1630	.123
	2.57	2.22	.0209	.0209	2530	.133
	3.34	2.58	.0162	.0162	4300	.142
	4.12	2.97	.0129	.0129	6500	.145
	5.50	3.80	.0091	.0091	11600	.145
	5.84	4.07	.0083	.0083	13000	.141

Table 3

(4)

ϕ	N RPS	$\frac{I_o}{I}$	d cm.	d/f_ϕ cm.	$\frac{N^2L^3\ \bar{\rho}}{\sigma}$	$\frac{N^{1.2}dL^{.8}\bar{\rho}^{.6}}{f_\phi\ \sigma^{.6}}$
		Probe 1 Methyl Iso-Butyl Ketone in H_2O				Impeller A4
.20	1.57	2.19	.0429	.0340	945	.120
	2.07	2.47	.0347	.0275	1630	.135
	2.57	2.79	.0285	.0226	2530	.144
	3.34	3.35	.0218	.0173	4300	.152
	4.12	3.95	.0173	.0137	6500	.154
	5.50	5.20	.0121	.0096	11600	.153
	5.84	5.40	.0116	.0092	13000	.156
.30	1.57	2.40	.0545	.0361	945	.128
	2.07	2.70	.0450	.0298	1630	.146
	2.57	3.11	.0362	.0240	2530	.153
	3.34	3.84	.0270	.0179	4300	.157
	4.12	4.65	.0209	.0138	6500	.155
	5.50	6.03	.0152	.0101	11600	.161
	5.84	6.67	.0135	.0089	13000	.151
.40	1.57	2.49	.0685	.0391	945	.138
	2.07	2.91	.0534	.0305	1630	.149
	2.57	3.38	.0429	.0244	2530	.156
	3.34	4.31	.0308	.0176	4300	.155
	4.12	5.25	.0240	.0137	6500	.154
	5.50	6.77	.0176	.0100	11600	.159
	5.84	7.47	.0158	.0090	13000	.153
		Probe 1 H_2O in Methyl Iso-Butyl Ketone				Impeller A4
.10	1.57	2.02	.0326	.0326	990	.119
	2.07	2.38	.0242	.0242	1710	.122
	2.57	2.71	.0195	.0195	2650	.128
	3.34	3.28	.0146	.0146	4500	.132
	4.12	3.83	.0118	.0118	6820	.137
	5.50	4.75	.0089	.0089	12100	.145
	5.84	5.06	.0082	.0082	13600	.144

Table 3

(5)

ϕ	N RPS	$\frac{I_o}{I}$	d cm.	d/f_ϕ cm.	$\frac{N^2 L^3 \bar{\rho}}{\sigma}$	$\frac{N^{1.2} d L^{.8} \bar{\rho}^{.6}}{f_\phi \sigma^{.6}}$
		Probe 1	H_2O in Methyl	Iso-Butyl	Ketone	Imepller A4
.20	1.57	2.85	.0358	.0284	990	.104
	2.07	3.45	.0272	.0216	1710	.109
	2.57	4.06	.0218	.0173	2650	.114
	3.34	4.96	.0168	.0133	4500	.120
	4.12	5.76	.0140	.0111	6820	.129
	5.50	7.19	.0107	.0085	12100	.139
	5.84	7.63	.0100	.0079	13600	.138
.30	1.57	3.57	.0389	.0265	990	.097
	2.07	4.27	.0305	.0202	1710	.102
	2.57	5.01	.0249	.0165	2650	.109
	3.34	6.20	.0192	.0127	4500	.115
	4.12	7.30	.0158	.0105	6820	.122
	5.50	9.02	.0124	.0082	12100	.134
	5.84	9.36	.0119	.0079	13600	.138
.40	1.57	4.14	.0424	.0242	990	.0885
	2.07	5.01	.0332	.0190	1710	.0960
	2.57	5.77	.0279	.0159	2650	.104
	3.34	7.09	.0218	.0125	4500	.112
	4.12	8.40	.0180	.0103	6820	.119
	5.50	9.72	.0153	.0087	12100	.142
	5.84	10.53	.0139	.0079	13600	.138
		Probe 1	Methyl	Iso-Butyl	Ketone in H_2O	Impeller A6
.10	1.57	1.58	.0439	.0439	945	.154
	3.34	2.58	.0161	.0161	4300	.141
	5.84	4.07	.0083	.0083	13000	.141
.20	1.57	1.85	.0600	.0476	945	.167
	2.07	2.25	.0408	.0324	1630	.159
	2.57	2.59	.0321	.0255	2530	.162
	3.34	3.35	.0217	.0172	4300	.151

Table 3

(6)

ϕ	N RPS	$\frac{I_o}{I}$	d cm.	d/f_ϕ cm.	$\frac{N^2L^3\bar{\rho}}{\sigma}$	$\frac{N^{1.2}dL^{.8}\bar{\rho}^{.6}}{f_\phi\ \sigma^{.6}}$
		Probe 1 Methyl	Iso-Butyl		Ketone in H_2O	Impeller A6
.20	4.12	4.07	.0166	.0132	6500	.149
	5.50	5.40	.0115	.0091	11600	.145
.30	1.57	2.10	.0695	.0460	945	.161
	2.07	2.54	.0497	.0329	1630	.161
	2.57	2.97	.0389	.0258	2530	.164
	3.34	3.84	.0270	.0179	4300	.157
	4.12	4.90	.0196	.0130	6500	.146
	5.50	6.47	.0139	.0092	11600	.146
.40	1.57	2.23	.0827	.0472	945	.167
	2.07	2.68	.0606	.0347	1630	.177
	2.57	3.16	.0472	.0270	2530	.173
	3.34	4.31	.0308	.0176	4300	.155
	4.12	5.43	.0231	.0132	6500	.148
	5.50	7.20	.0164	.0094	11600	.148
		Probe 1 H_2O in Methyl	Iso-Butyl		Ketone	Impeller A6
.10	1.57	1.78	.0425	.0425	990	.156
	2.07	2.10	.0303	.0303	1710	.153
	2.57	2.42	.0234	.0234	2650	.154
	3.34	2.95	.0171	.0171	4500	.154
	4.12	3.47	.0135	.0135	6820	.156
	5.50	4.20	.0104	.0104	12100	.170
.20	1.57	2.36	.0490	.0389	990	.142
	2.07	3.06	.0324	.0257	1710	.130
	2.57	3.57	.0259	.0206	2650	.135
	3.34	4.60	.0185	.0147	4500	.132
	4.12	5.40	.0151	.0120	6820	.139
	5.50	6.70	.0116	.0090	12100	.150

Table 3

(7)

ϕ	N RPS	$\frac{I_o}{I}$	d cm.	d/f_ϕ cm.	$\frac{N^2L^3\,\bar{\rho}}{\sigma}$	$\frac{N^{1.2}dL^{.8}\,\bar{\rho}^{.6}}{f_\phi\,\sigma^{.6}}$
		Probe 1 H_2O in Methyl Iso-Butyl Ketone				Impeller A6
.30	1.57	2.97	.0506	.0336	900	.123
	2.07	3.91	.0343	.0227	1710	.115
	2.57	4.60	.0278	.0184	2650	.121
	3.34	5.84	.0206	.0136	4500	.122
	4.12	6.89	.0170	.0112	6820	.130
	5.50	8.41	.0134	.0089	12100	.145
.40	1.57	3.35	.0566	.0324	990	.119
	2.07	4.35	.0398	.0228	1710	.115
	2.57	5.16	.0320	.0183	2650	.121
	3.34	6.70	.0241	.0138	4500	.124
	4.12	7.88	.0193	.0110	6820	.127
	5.50	9.72	.0153	.0087	12100	.142
		Probe 3 Methyl Iso-Butyl Ketone in H_2O				Impeller B4
.20	1.57	1.66	.0420	.0334	6500	.195
	2.47	2.34	.0206	.0164	16100	.166
.30	1.57	1.84	.0493	.0327	6500	.192
	2.47	2.56	.0266	.0176	16100	.178
.40	1.57	1.91	.0607	.0347	6500	.204
	2.47	2.72	.0321	.0183	16100	.185
		Probe 3 H_2O in Methyl Iso-Butyl Ketone				Impeller B4
.20	1.57	2.88	.0191	.0152	6800	.0915
	2.47	4.03	.0119	.0094	16800	.0977
.30	1.57	3.36	.0229	.0152	6800	.0915
	2.47	4.70	.0146	.0096	16800	.0998

Table 4

Effect of Volume Fraction in Liquid-Liquid Mixtures

$d/d_{.1} = f_{\phi}$

Dispersed Phase	Continuous Phase	Impeller Number	N RPS	$\phi = .2$ f_{ϕ} Avg. f_{ϕ}	$\phi = .3$ f_{ϕ} Avg. f_{ϕ}	$\phi = .4$ f_{ϕ} Avg. f_{ϕ}
CCl_4	Water	A3	2.57	1.11	1.34	
			4.12	1.07	1.51	
			6.57	1.36	1.62	
		A5	4.12	1.24	1.64	
			6.57	1.31(1.22)	1.70 (1.56)	
Iso-Octane	Water	A3	2.57	1.35	1.67	
			4.12	1.16	1.39	
			6.57	1.25(1.25)	1.39 (1.48)	
Water	Kerosene	A3	2.57	1.27	1.57	
			4.12	1.30	1.73	
			6.57	1.43	1.90	
		A5	2.57	1.38	1.77	
			4.12	1.33	1.69	
			6.57	1.53(1.37)	2.03 (1.45)	
Methyl Iso-Butyl Ketone	Water	A4	1.57	1.43	1.82	2.29
			2.07	1.39	1.81	2.14
			2.57	1.36	1.73	2.04
			3.34	1.34	1.66	1.89
			4.12	1.34	1.62	1.87
			5.50	1.33	1.68	1.94
			5.84	1.40	1.62	1.90
		A6	1.57	1.37	1.59	1.89
			3.34	1.35(1.37)	1.69 (1.69)	1.93 (1.99)
Water	Methyl Iso-Butyl Ketone	A4	1.57	1.10	1.19	1.30
			2.07	1.12	1.26	1.37
			2.57	1.12	1.27	1.43
			3.34	1.15	1.31	1.50
			4.12	1.19	1.35	1.54
			5.50	1.20	1.40	1.55
			5.84	1.22	1.45	1.70
		A6	1.57	1.16	1.19	1.34
			2.07	1.07	1.13	1.32
			2.57	1.11	1.19	1.37
			3.34	1.08	1.20	1.41
			4.12	1.12	1.26	1.43
			5.50	1.12(1.14)	1.29 (1.27)	1.48 (1.44)

Table 5
Power in Liquid-Liquid Systems

System	Impeller	ø	N RPS	Lb. Force on Lever Arm	P_o
MiBK in H_2O Unbaffled	B3	0	1.57	2.20	6.45
			2.57	6.30	6.90
			4.12	15.00	6.55
		.10	1.57	2.20	6.59
			2.57	6.30	7.03
			4.12	15.00	6.66
		.20	1.57	2.12	6.50
			2.57	5.95	6.78
			4.12	14.80	6.66
		.40	1.57	1.99	6.41
			2.57	5.85	6.97
			4.12	13.80	6.47
H_2O in MiBK Unbaffled	B3	.10	1.57	1.83	6.53
			2.57	5.30	7.03
			4.12	11.0	5.78
		.20	1.57	1.87	6.53
			2.57	5.33	6.91
			4.12	12.6	6.47
		.40	1.57	1.87	6.21
			2.57	5.33	6.60
			4.12	13.10	6.41
MiBK in H_2O Unbaffled	B4	.10	1.57	1.73	4.96
			2.57	4.85	5.15
			4.12	12.00	5.03
		.20	1.57	1.69	4.96
			2.57	4.63	5.03
			4.12	11.70	5.03
	B4	.40	1.57	1.64	4.96
			2.57	4.55	5.15
			4.12	11.40	4.90
H_2O in MiBK Unbaffled	B4	.10	1.57	1.43	4.84
			2.57	4.00	5.09
			4.12	10.30	5.09
		.20	1.57	1.43	4.70
			2.57	4.05	5.03
			4.12	10.40	5.03
		.40	1.57	1.51	4.71
			2.57	4.27	5.09
			4.12	10.70	5.03

Table 5
(2)

System	Impeller	Ø	N RPS	Lb. Force on Level Arm	P_o
MiBK in H_2O Unbaffled	B2	.10	1.57	.39	5.90
			2.57	1.21	6.90
			4.12	3.40	7.60
			6.57	8.45	5.72
		.20	1.57	.37	5.78
			2.57	1.19	6.85
			4.12	3.35	7.80
			6.57	8.40	5.78
		.40	1.57	.35	5.85
			2.57	1.15	6.98
			4.12	3.25	7.66
			6.57	8.10	5.85
H_2O in MiBK Unbaffled	B2	.10	1.57	.28	5.21
			2.57	1.00	6.79
			4.12	2.85	7.66
			6.57	7.25	5.85
		.20	1.57	.32	5.71
			2.57	1.03	6.79
			4.12	2.90	7.60
			6.57	7.50	5.90
		.40	1.57	.33	5.60
			2.57	1.07	6.79
			4.12	3.00	7.54
			6.57	7.65	5.78
H_2O in CCl_4 Baffled	A2	.10	4.12	.85	21.4
			6.57	2.20	22.3
		.20	4.12	.75	19.7
			6.57	2.10	22.1
		.40	4.12	.70	20.0
			6.57	1.85	21.2
CCl_4 in H_2O Baffled	A2	.10	4.12	.53	19.3
			6.57	1.40	20.6
		.20	4.12	.55	19.0
			6.57	1.55	21.5
		.40	4.12	.62	19.4
			6.57	1.65	20.7
H_2O in CCl_4 Baffled	A4	.10	1.57	.65	19.0
			2.57	1.85	21.0
			4.12	4.90	20.6
			6.57	12.30	20.8
		.20	1.57	.62	18.7
			2.57	1.70	20.1
			4.12	4.65	20.2
			6.57	11.50	20.2
		.40	1.57	.53	17.5
			2.57	1.55	19.9
			4.12	4.10	19.4
			6.57	10.60	20.2

Table 5
(3)

System	Impeller	ø	N RPS	Lb. Force on Level Arm	P_o
CCl_4 in H_2O Baffled	A4	.10	1.57	.39	16.1
			2.57	1.20	19.8
			4.12	3.30	20.0
			6.57	8.60	21.0
		.20	1.57	.39	15.6
			2.57	1.25	19.6
			4.12	3.45	19.8
			6.57	9.00	20.9
		.40	1.57	.49	17.7
			2.57	1.35	19.1
			4.12	3.75	19.5
			6.57	9.75	20.5
H_2O in CCl_4 Baffled	A3	.10	2.57	1.40	18.0
			4.12	3.80	18.8
			6.57	9.95	19.7
		.20	2.57	1.35	18.0
			4.12	3.65	18.8
			6.57	9.45	19.5
		.40	2.57	1.25	18.2
			4.12	3.25	18.2
			6.57	8.45	18.9
CCl_4 in H_2O Baffled	A3	.10	2.57	.97	18.0
			4.12	2.65	19.0
			6.57	6.90	19.8
		.20	2.57	1.00	17.7
			4.12	2.75	18.7
			6.57	7.20	19.6
		.40	2.57	1.13	18.0
			4.12	2.95	18.1
			6.57	7.70	18.9
H_2O in MiBK Baffled	A3	.10	1.57	.37	19.9
			2.57	.93	18.6
			4.12	2.45	19.1
			6.57	6.30	19.4
		.20	1.57	.36	19.8
			2.57	.93	19.1
			4.12	2.40	19.2
			6.57	6.15	19.4
		.40	1.57	.33	19.0
			2.57	.85	18.2
			4.12	2.25	18.8
			6.57	5.75	19.0

Table 5
(4)

System	Impeller	Ø	N RPS	Lb. Force on Level Arm	P_o
MiBK in H_2O	A3	.10	1.57	.30	19.4
Baffled			2.57	.77	18.4
			4.12	2.00	18.7
			6.57	5.30	19.6
		.20	1.57	.30	18.9
			2.57	.78	18.2
			4.12	2.05	18.7
			6.57	5.35	19.3
		.40	1.57	.31	18.7
			2.57	.80	17.9
			4.12	2.10	18.3
			6.57	5.50	18.9

Table 6

Mixing Index Data

$$X = \frac{NL\,(We^{.6}\ \rho_m)^{1/2}}{(.084\, f_\phi |\rho_m - \rho_D| gL)^{1/2}} = \frac{NL\ \rho_m^{1/2}}{(|\rho_m - \rho_D|\ dg)^{1/2}}$$

$$Y = (LW/TH)\ X$$

System	Impeller	N RPS	i_m at Points in % Ø	1	2	3	4	5	6	I_m Avg.	X	Y
Water in CCl_4	A2	2.57	.1	3.1	65.0	69.0	5.2	90.2	65.0	49.6	10.6	.540
		4.12		94.9	96.7	92.0	86.0	70.8	75.7	86.0	22.7	1.17
		2.57	.2	0	23.0	25.0	0	61.0	29.0	23.0	9.87	.504
		4.12		74.9	97.0	96.0	57.3	76.6	84.7	81.1	21.1	1.07
		2.57	.4	0	84.3	43.6	0	4.9	47.0	30.0	9.30	.475
		4.12		94.0	95.0	91.8	86.9	84.9	86.9	89.9	19.8	1.01
	A3	1.57	.1	11.2	66.5	65.0	8.7	97.5	98.5	57.9	8.35	.64
		1.57	.2	0	49.0	56.1	0	83.2	64.5	42.1	7.75	.593
		2.57		83.1	98.7	98.4	69.2	74.3	86.0	85.0	17.1	1.31
		1.57	.4	0	40.8	54.0	0	12.6	68.8	29.4	7.30	.559
		2.57		99.0	99.0	95.0	94.0	93.7	96.9	96.3	16.1	1.23
	A4	1.57	.1	75.3	99.7	98.5	74.0	56.4	81.0	80.8	6.75	.815
		1.57	.2	36.8	79.0	91.9	2.9	70.2	81.5	60.4	6.26	.757
		1.57	.4	0	96.4	85.9	0	50.3	80.2	52.1	5.80	.701
Methyl Iso-Butyl Ketone in Water	A1	4.12	.3	0		0	0		0	0	13.6	.347
		6.57		0		56.0	0		71.0	31.7	28.0	.715
		4.12	.5	0	0		0	0		0	15.8	.396
		6.57		0	22.4		0	53.5		19.0	32.2	.781
	A2	1.57	.3	0		16.0	2.0		17.0	8.75	7.65	.390
		2.57		88.0		87.2	9.0		96.0	70.0	16.2	.826
		1.57	.5	0	75.6		0	0		18.9	8.83	.450
		2.57		87.0	93.5		4.0	75.6		65.0	18.4	.938
Water in Methyl Iso-Butyl Ketone	A1	4.12	.3	0		27.0	0		12.5	9.9	13.2	.337
		6.57		0		83.5	0		73.5	39.2	26.8	.683
	A2	1.57	.3	0		29.0	0		0	7.25	7.45	.380
		2.57		86.5		95.5	65.0		85.0	83.0	15.4	.785

At points where no i_m indicated no samples were taken because of proximity of interface.

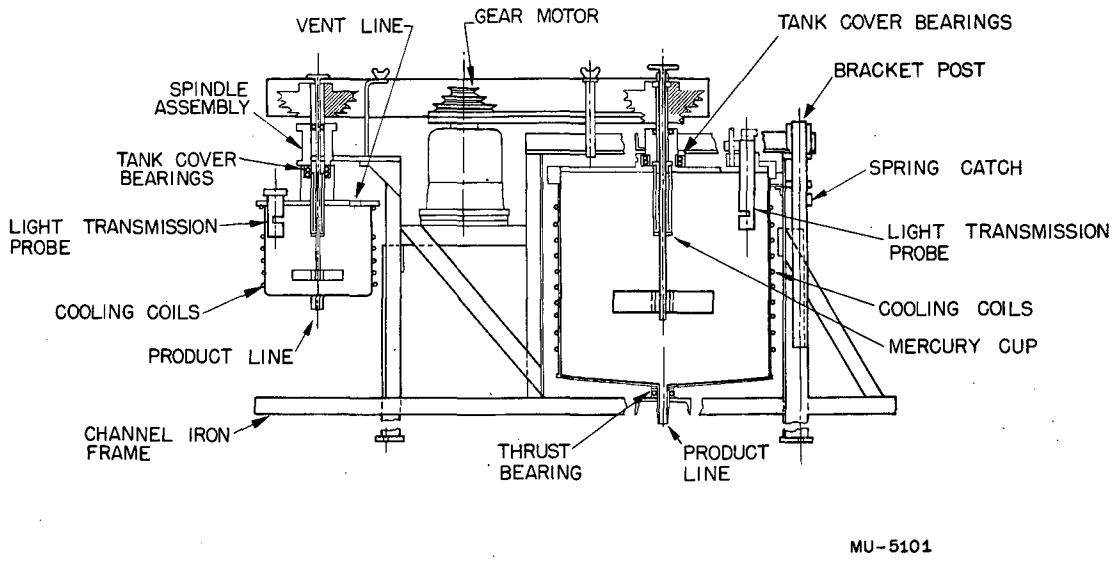

Figure 1. Agitation Apparatus.

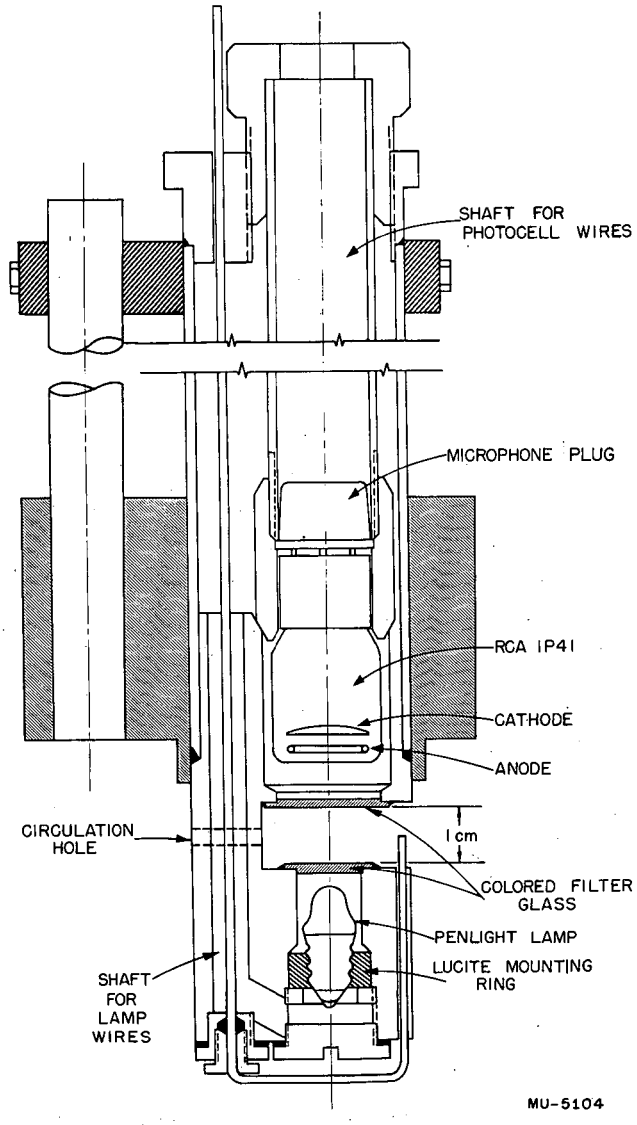

Fig. 2. Photoelectric Light Transmission Probe.

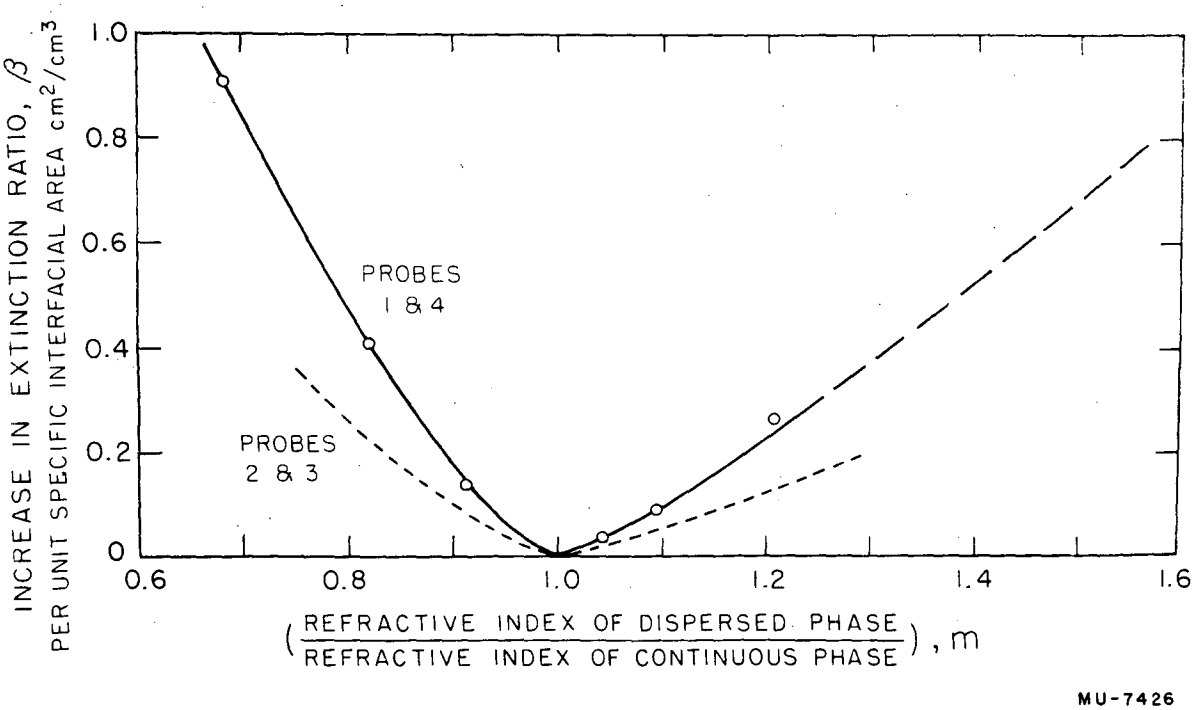

Fig. 3. Effect of Refractive Index Ratio on Light Transmission.

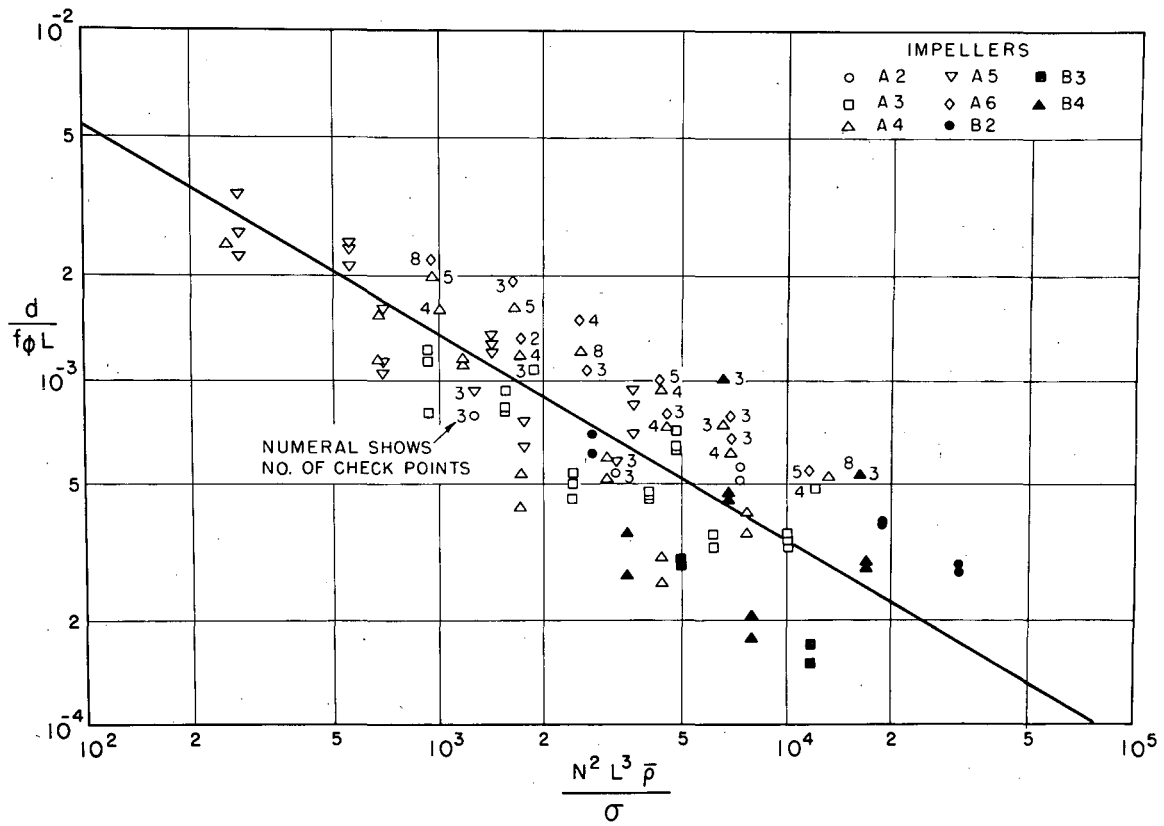

Fig. 4. Diameter / Weber - Number Relation for Various Agitator Dimensions.

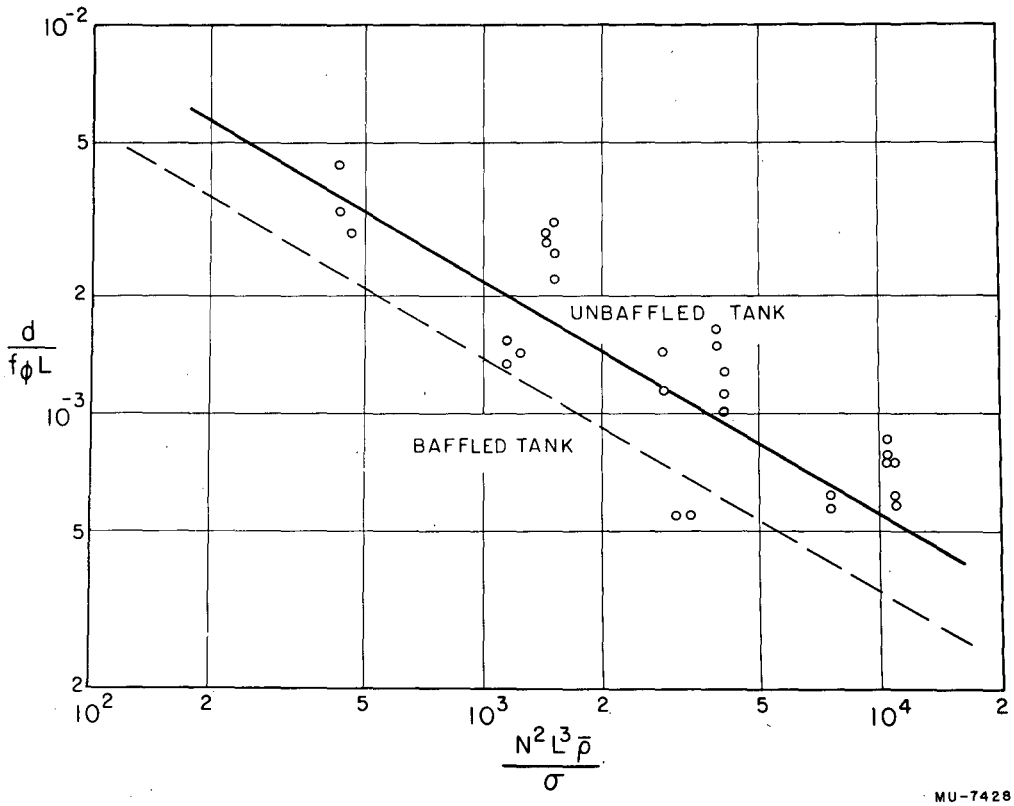

Fig. 5. Mean Drop Diameter in Unbaffled Tank.

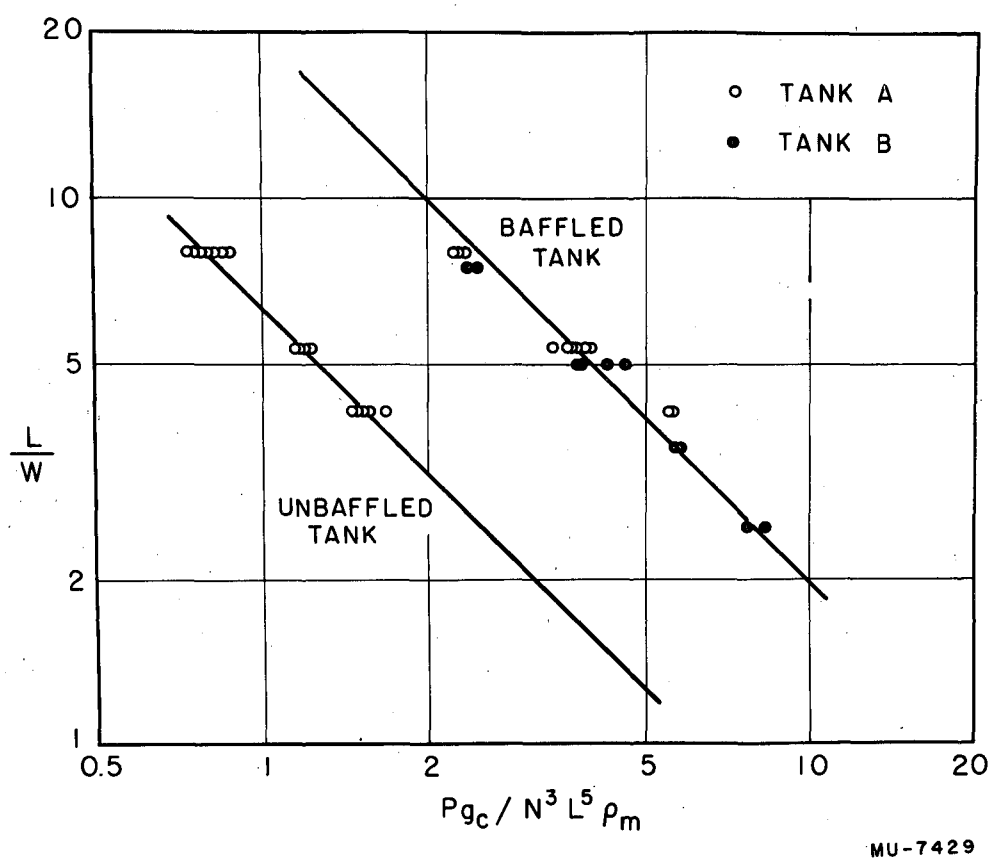

Fig. 6. Effect of Impeller Diameter-to-width Ratio Upon Power Consumption.

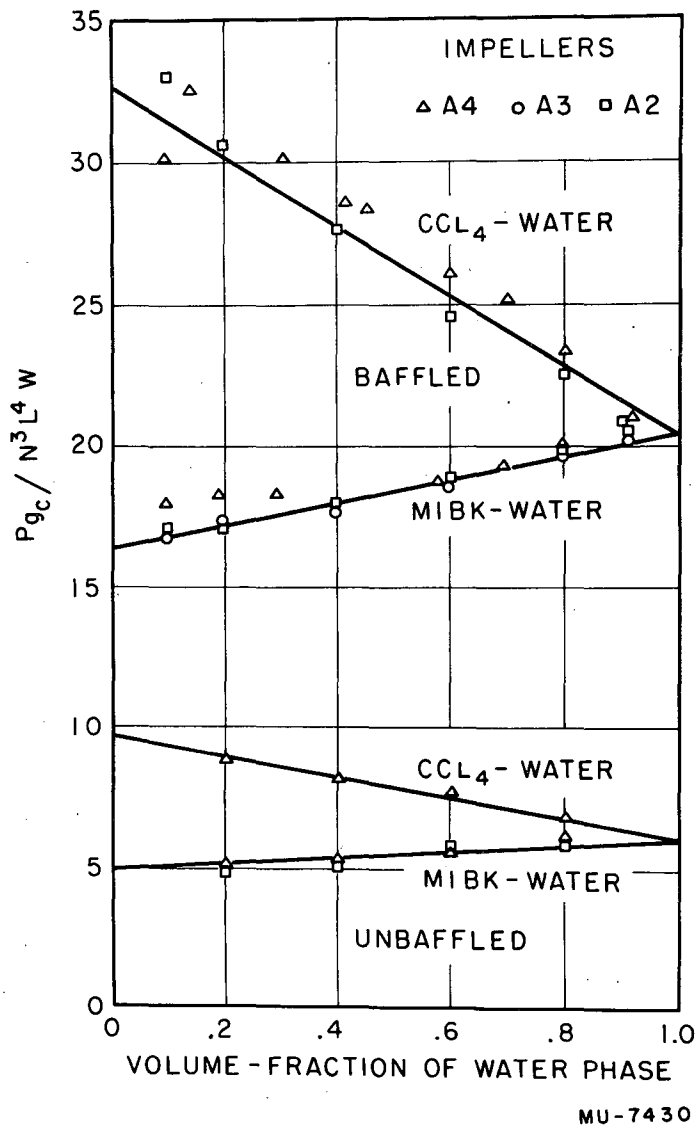

Fig. 7. Power Consumption of Liquid-Liquid Mixtures.

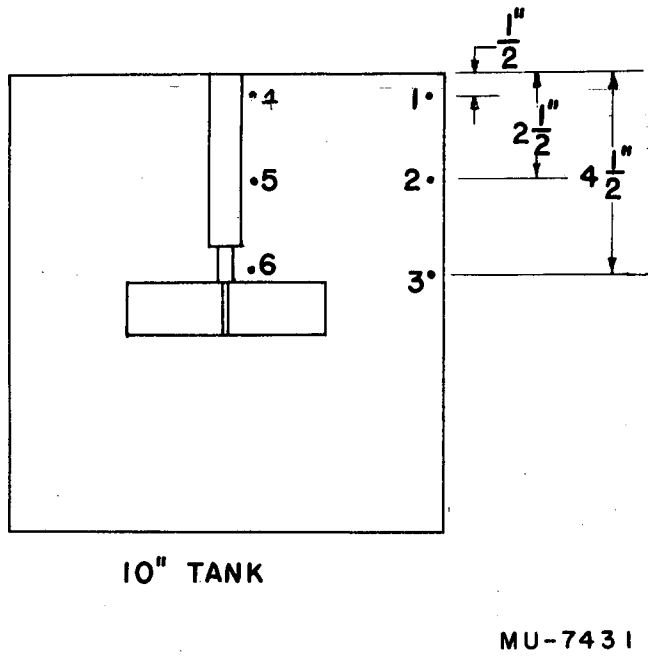

Fig. 8. Mixed Index Sampling Points.

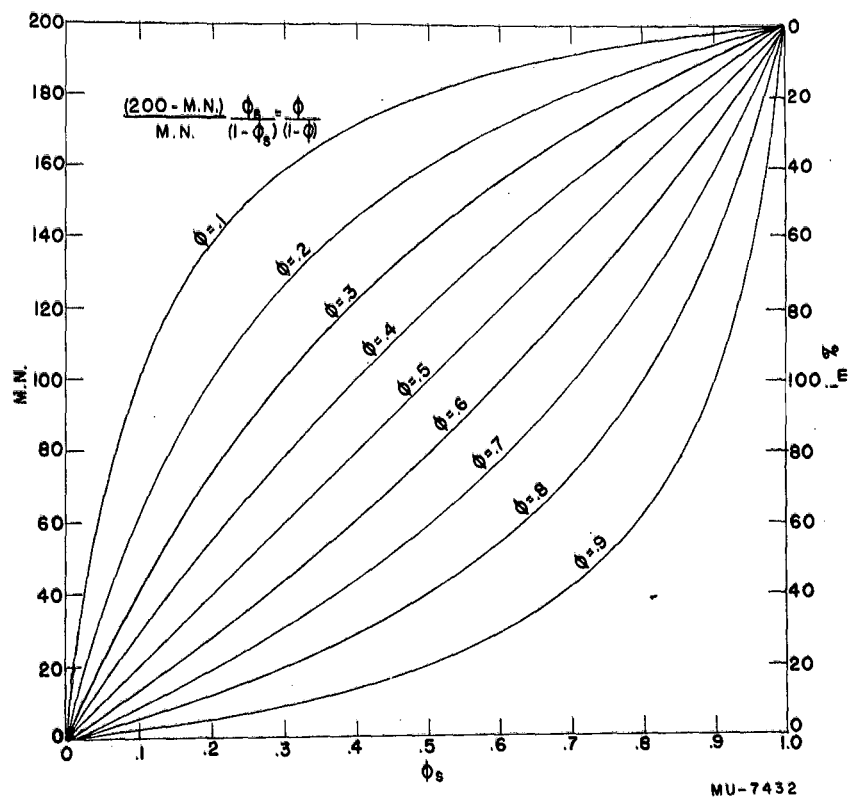

Fig. 9. Mixing Index vs. ϕ at Sampling Points.

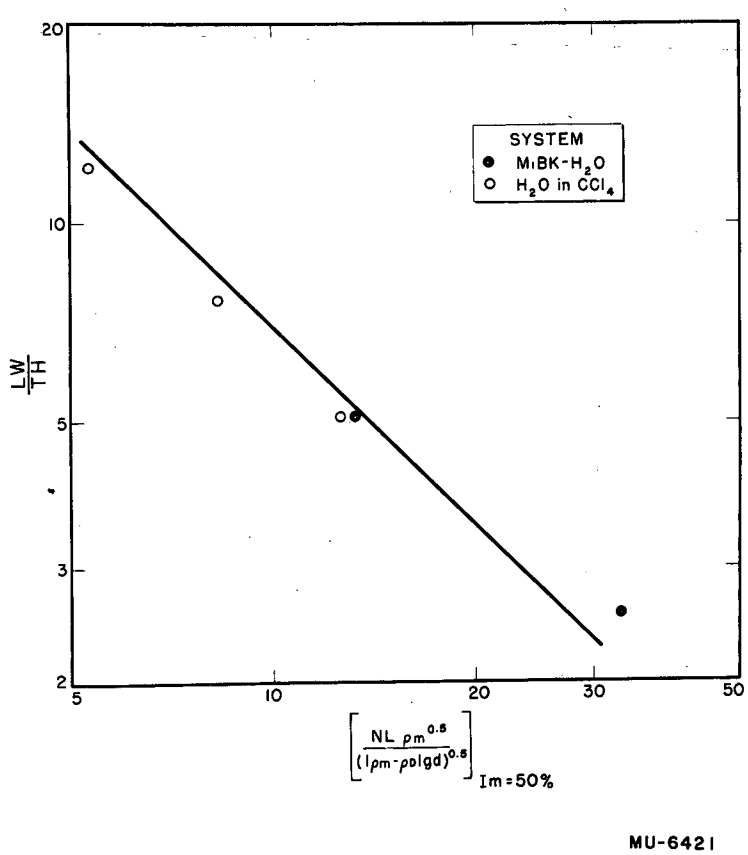

Fig. 10. Settling Group vs. Geometric Factor.

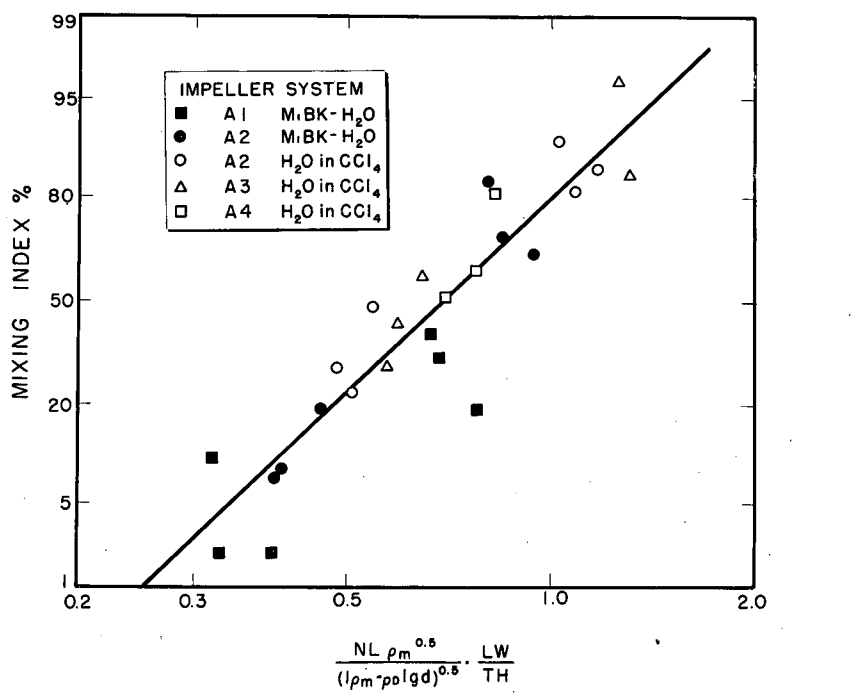

MU-6422

Fig. 11. Tentative Mixing Index Correlation.